

## PYROSTATINS A AND B, NEW INHIBITORS OF *N*-ACETYL- $\beta$ -D-GLUCOSAMINIDASE, PRODUCED BY *Streptomyces* sp. SA-3501

TAKAYUKI AOYAMA, FUKIKO KOJIMA, CHIAKI IMADA,  
YASUHIKO MURAOKA, HIROSHI NAGANAWA, YOSHIRO OKAMI,  
TOMIO TAKEUCHI and TAKAAKI AOYAGI\*<sup>†</sup>

*Institute of Microbial Chemistry, 3-14-23 Kamiosaki,  
Shinagawa-ku, Tokyo 141, Japan*

<sup>†</sup>*Showa College of Pharmaceutical Sciences, Machida-shi, Tokyo 194, Japan*

(Received 3 October 1994)

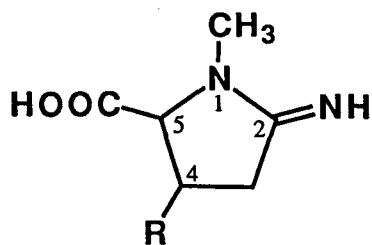
Pyrostatins A and B, new inhibitors of *N*-acetyl- $\beta$ -D-glucosaminidase (GlcNAc-ase), have been purified from the culture broth of *Streptomyces* sp. SA-3501 isolated from a marine environment. They were purified by chromatography on Dowex 50W, silica gel and Capcell Pak C<sub>18</sub> (HPLC) followed treatment with active carbon and then isolated as white powders. The structures of pyrostatins A and B were determined by NMR studies to be 4-hydroxy-2-imino-1-methylpyrrolidine-5-carboxylic acid and 2-imino-1-methylpyrrolidine-5-carboxylic acid, respectively. They were competitive with the substrate, and the inhibition constants ( $K_i$ ) of pyrostatins A and B were  $1.7 \times 10^{-6}$  M and  $2.0 \times 10^{-6}$  M respectively.

KEY WORDS: *N*-acetyl- $\beta$ -D-glucosaminidase, inhibitor, pyrostatin, *Streptomyces*, marine microbe

### INTRODUCTION

*N*-acetyl- $\beta$ -D-glucosaminidase (GlcNAc-ase, EC 3.2.1.30) catalyzes the hydrolysis of glycosidic linkages as an exoglycosidase and releases *N*-acetyl- $\beta$ -D-glucosamine from glycoproteins. In several diseases such as diabetes mellitus,<sup>1</sup> leukemia<sup>2</sup> and cancer,<sup>3</sup> GlcNAc-ase activity in serum has been reported to increase, especially in the process of tumor cell invasion which is one of the stages of metastasis, GlcNAc-ase activity of the tumor plays an important role in the hydrolysis of glycoconjugates present in extracellular matrix.<sup>4</sup> Thus, a potent inhibitor of this enzyme is of considerable interest for elucidating the cause and process of the above diseases. We have previously isolated nagstatin from the culture broth of *Streptomyces amakusaensis* MG846-fF3 as a novel inhibitor of GlcNAc-ase.<sup>5,6</sup> In the course of our continuing screening for new inhibitors of GlcNAc-ase, we discovered pyrostatins A and B as specific inhibitors as shown in Figure 1. In this communication, we report the taxonomy of

\* Correspondence



**Pyrostatin A** R=OH

**Pyrostatin B** R=H

FIGURE 1 Structures of pyrostatins A and B.

the strain, production, isolation, structure determination and biological activities of the inhibitors.

## MATERIALS AND METHODS

### Chemicals

Chemicals employed were as follows: active carbon was from Wako Pure Chemical Industries, Ltd., Osaka, Japan; Dowex 50W and Dowex 1 from Muromachi Kagaku Kogyo Kaisha, Ltd., Tokyo, Japan; Silica gel 60 and TLC-plate Silica gel F<sub>254</sub> (0.25 mm thickness) from E. Merck, Darmstadt, FRG; Sephadex G-10 from Pharmacia Fine Chemicals AB, Uppsala, Sweden; packed column of Capcell Pak C<sub>18</sub> from Shiseido Co, Tokyo, Japan; *p*-nitrophenyl-*N*-acetyl- $\beta$ -D-glucosaminide (NP-GlcNAc) from Sigma Chemical Co., St. Louis, U.S.A. All other chemicals were of analytical grade.

### Enzymes

GlcNAc-ase was prepared from hog kidney according to the method described by Tarentino *et al.*<sup>7</sup> and partially purified enzyme was used in the assay.

### Assay for *N*-Acetyl- $\beta$ -D-glucosaminidase (GlcNAc-ase) and Inhibitory Activity

The activity of GlcNAc-ase was determined colorimetrically by measuring the amount of *p*-nitrophenol liberated when NP-GlcNAc was used as a substrate.<sup>7</sup> The reaction mixture (total 200  $\mu$ l) contained 100  $\mu$ l of 0.1 M sodium citrate buffer (pH 4.5), 30  $\mu$ l of 20 mM NP-GlcNAc and water or aqueous solution containing the test compound. The mixture was incubated at 37°C for 3 min and 10  $\mu$ l of GlcNAc-ase solution was added. After 30 min, 100  $\mu$ l of 0.6 M glycine-sodium hydroxide buffer (pH 10.5) was added to the reaction to terminate it. The absorbance at 405 nm of the liberated nitrophenol was measured by microplate reader model 3550 (BIO-RAD).

The percent inhibition was calculated by the formula  $(A-B)/A \times 100$ , where A is the amount of nitrophenol liberated by the enzyme without an inhibitor and B is that with an inhibitor.  $IC_{50}$  value is the concentration of inhibitor to reduce the enzyme activity by 50%.

### *Microorganism*

Strain SA-3501 was isolated from a marine sediment collected from Otsuchi Bay (Depth, 105 m), Iwate Prefecture, Japan and has been deposited in the Fermentation Research Institute, Agency of Industrial Science and Technology, Ministry of International Trade and Industry, Tsukuba, Japan, under the accession No. FERM P-14182.

### *Taxonomic Characterization*

Morphological and physiological properties of the strain were examined according to Shirling and Gottlieb<sup>8</sup> after cultivation at 27°C for 2 weeks. The Color Harmony Manual (4th Ed., 1958, Container Corporation of America, Chicago, Illinois) was used to identify the color of the mycelium and soluble pigment.

### *Production of Pyrostatins A and B*

A loopful of slant culture of the strain SA-3501 was inoculated into 110 ml of a production medium consisting of soluble starch 2.0%, glucose 1.0%, Bacto-yeast extract (Difco) 0.5%, Trypticase (BBL Co., Ltd.) 0.5%,  $CaCO_3$  0.2% with a quarter strength artificial seawater (Jamarin Lab., Osaka) in a 500-ml baffled Erlenmeyer flask, and incubated at 27°C for 2 days on a rotary shaker (180 rpm). After incubation, 2 ml of this seed culture was transferred to 110 ml of the fresh medium in the same type of flask and cultured for 4 days under the same conditions.

### *Isolation of Pyrostatins A and B*

The culture broth was filtered through Celite and the culture filtrate was percolated through a column (7 × 23 cm) packed with active carbon for decolorization. The effluent was added to a Dowex 50W ( $H^+$ ) column (7.5 × 40 cm) and eluted with 1.5 N  $NH_4OH$ . The active fractions were concentrated and lyophilized to give a brownish powder. The crude powder was dissolved in  $H_2O$  and the solution was subjected to a Dowex 1 ( $AcO^-$ ) column (4 × 48 cm) chromatography and developed with  $H_2O$ . The eluate was concentrated and lyophilized to give a brownish powder. The powder was suspended in a solvent mixture of BuOAc-BuOH-AcOH- $H_2O$  (1:4:1:1) and charged to a silica gel column (4 × 52 cm). After washing the column with the same solvent mixture, the active substances were eluted with a solvent mixture of BuOH-AcOH- $H_2O$  (4:1:1). The eluted fractions containing pyrostatins were concentrated and lyophilized to give a slightly brownish powder. The powder was dissolved in a small volume of  $H_2O$ , and the solution was subjected to Sephadex G-10 column (4.5 × 125 cm) chromatography and eluted with  $H_2O$ . The eluate was concentrated and lyophilized to give a white powder. The powder was further purified by reversed-phase

HPLC using a Capcell Pak C<sub>18</sub> column (2 × 25 cm, flow rate 8 ml/minute) with H<sub>2</sub>O. The active fractions to appear first consisted of pyrostatin A, and the active fractions coming next comprised pyrostatin B. Each eluate was concentrated and lyophilized to give a white powder.

#### *Analytical Instruments*

HPLC was performed by a Gilson's system equipped with a Waters 991J photodiode array detector. Melting points were taken using a Yanaco MP-500D apparatus and were uncorrected. Optical rotations were measured on a Perkin-Elmer 241 polarimeter using micro-cell (light path 10 cm). UV spectra and IR spectra were recorded on a Hitachi U-3210 and a Hitachi 260-10 spectrophotometer, respectively. Mass spectra were obtained on a JEOL JMS-SX 102 mass spectrometer. NMR spectra were recorded on a JEOL JNM-A500 NMR spectrometer with <sup>1</sup>H NMR at 500 MHz and <sup>13</sup>C NMR at 125 MHz.

## RESULTS AND DISCUSSION

### *Taxonomic Characterization of the Producing Strain*

Strain SA-3501 had substrate and aerial hyphae which ranged about 1 μm in diameter. Mature spores occurred in spiral chains and the spores were cylindrical with smooth surface. No whirl-formation as well as no sporangia were observed. Aerial mass color of the colony was white to bluish white. The reverse side color of the colony was yellowish gray to pale brown. Soluble pigments were not formed on all the media. The whole-cell hydrolysate of the strain showed that it contained LL-diaminopimelic acid. Based on its characteristics, strain SA-3501 was considered to belong to the genus *Streptomyces*.

### *Production and Isolation of Pyrostatins A and B*

The strain of *Streptomyces* sp. SA-3501 was cultured in Erlenmeyer flasks at 27°C on a rotary shaker, and the time course of the production of the inhibitor, fluctuation of pH and residual glucose in the broth were determined. The maximum production was obtained after 4 days cultivation and this level was little maintained thereafter. However, there was little variation of the pH in the broth which remained between 7.5 and 8.0 throughout the time of the experiment. The amount of residual glucose was decreased as the production of the inhibitor increased (Figure 2). As shown in Figure 3, pyrostatins A and B were isolated from the culture filtrate (14 liters), and the total yields were 617.1 mg and 295.9 mg, respectively. The purity of each preparation was confirmed by TLC and HPLC.

### *Structure Determinations of Pyrostatins A and B*

The physico-chemical properties of pyrostatins A and B are summarized in Table 1. They are soluble in water, dimethyl sulfoxide and methanol but insoluble in chloroform.

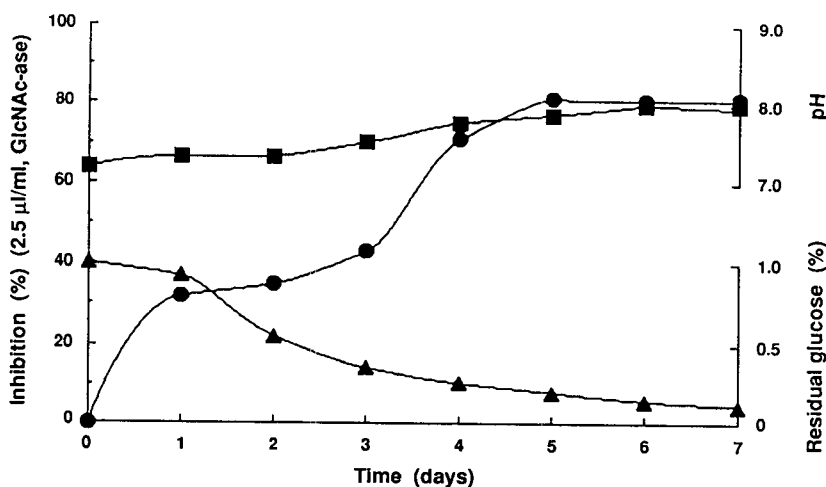


FIGURE 2 Time course of pyrostatins production by *Streptomyces* sp. SA-3501. ● Inhibitors, ■ pH of the broth, ▲ residual glucose in the broth.

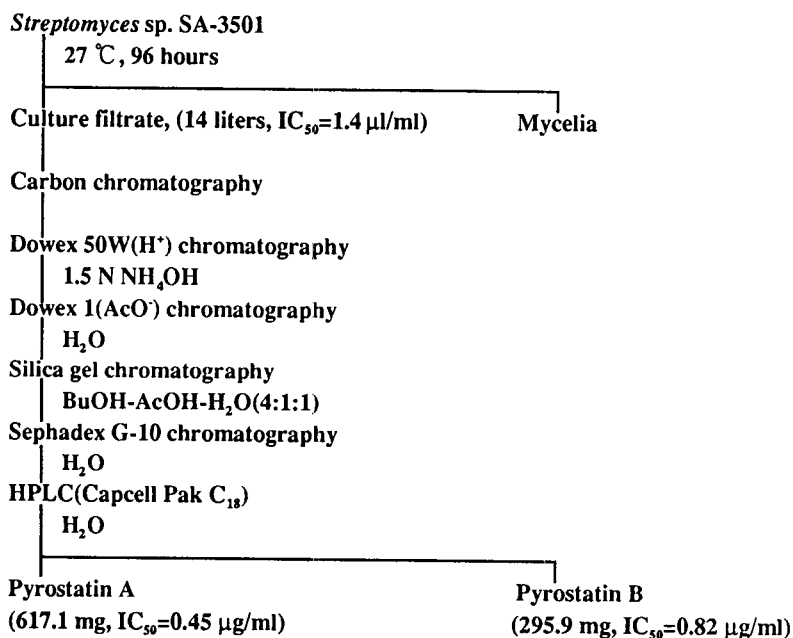


FIGURE 3 Isolation procedure for pyrostatins A and B.

TABLE 1  
Physico-chemical properties of pyrostatins A and B.

	Pyrostatin A	Pyrostatin B
Appearance	White powder	White powder
MP	92~94°C	93~95°C
$[\alpha]_D$ (c 0.5 H <sub>2</sub> O)	+125.4 (29°C)	+98.4 (30°C)
FAB-MS ( <i>m/z</i> , Pos.)	159 (M+H) <sup>+</sup>	143 (M+H) <sup>+</sup>
MW	158	142
HRFAB-MS ( <i>m/z</i> )		
Found:	159.0770 (M+H) <sup>+</sup>	143.0821 (M+H) <sup>+</sup>
Calcd:	159.0767 for C <sub>6</sub> H <sub>11</sub> N <sub>2</sub> O <sub>3</sub>	143.0819 for C <sub>6</sub> H <sub>11</sub> N <sub>2</sub> O <sub>2</sub>
Molecular formula	C <sub>6</sub> H <sub>10</sub> N <sub>2</sub> O <sub>3</sub>	C <sub>6</sub> H <sub>10</sub> N <sub>2</sub> O <sub>2</sub>
UV $\lambda$ max nm ( $\epsilon$ ) in H <sub>2</sub> O	End absorption	205 (4771)
IR $\nu$ max cm <sup>-1</sup> (KBr)	3405, 3070, 2820, 1670, 1625, 1405, 1370, 1330, 1100, 915	3400, 3050, 2800, 1665, 1615, 1400, 1315, 1210, 1145, 780
Rf value <sup>a</sup>	0.35	0.35
Rm value (alanine = 1.0) <sup>b</sup>	1.05	1.05
Color reaction	Greig-Leaback	Greig-Leaback
Solubility	Soluble: H <sub>2</sub> O, DMSO, MeOH Insoluble: CHCl <sub>3</sub>	Soluble: H <sub>2</sub> O, DMSO, MeOH Insoluble: CHCl <sub>3</sub>

<sup>a</sup>Silica gel TLC: BuOH: AcOH:H<sub>2</sub>O (2:1:1)

<sup>b</sup>HVPE: HCOOH-AcOH-H<sub>2</sub>O (1:3:36, pH 1.6), 800 V, 10 min.

The molecular weight and formula of pyrostatin A were elucidated as C<sub>6</sub>H<sub>10</sub>N<sub>2</sub>O<sub>3</sub> (MW 158) from the FAB-MS peak at *m/z* 159 (M+H)<sup>+</sup>, HRFAB-MS [found: *m/z* 159.0770 (M+H)<sup>+</sup>, calcd: *m/z* 159.0767 for C<sub>6</sub>H<sub>11</sub>N<sub>2</sub>O<sub>3</sub>] and <sup>1</sup>H and <sup>13</sup>C NMR spectra of pyrostatin A (Tables 2 and 3). The UV spectrum showed end absorption in H<sub>2</sub>O. The IR spectrum (KBr) showed the presence of hydroxy group (3405 cm<sup>-1</sup>), a N-CH<sub>3</sub> bond (2820 cm<sup>-1</sup>), a C=N bond (1670 cm<sup>-1</sup>) and a carboxylate anion (1625 and 1405 cm<sup>-1</sup>) which were supported by <sup>13</sup>C NMR signals at  $\delta_c$  161.3 (C-2) and 175.1 (C-7) ppm.

The <sup>1</sup>H-<sup>1</sup>H COSY spectrum and spin decoupling experiments of pyrostatin A revealed two *vicinal*-spin spin couplings among 3-H<sub>2</sub> at  $\delta_H$  3.31, 3.45 ppm, 4-H at  $\delta_H$  4.54 ppm and 5-H at  $\delta_H$  4.05 ppm. A long-range spin coupling between 3-H at  $\delta_H$  3.45 ppm and 5-H at  $\delta_H$  4.05 ppm was also observed.

As shown in Figure 4, the HMBC (heteronuclear multiple bond connectivity) spectrum of pyrostatin A revealed that the methyl protons at  $\delta_H$  2.30 (6-H<sub>3</sub>) coupled to the carbon signal at  $\delta_c$  161.3 (C-2) ppm. The methylene proton at  $\delta_H$  3.45 (3-H) ppm correlated with three carbons at  $\delta_c$  161.3 (C-2), 60.2 (C-4) and 60.6 (C-5) ppm. The methine proton at  $\delta_H$  4.05 (5-H) ppm coupled to four carbons at  $\delta_c$  161.3

TABLE 2  
<sup>1</sup>H NMR data of pyrostatins in D<sub>2</sub>O.

Proton	$\delta_{\text{H}}$ ppm ( <i>J</i> in Hz, 500 MHz)		
	Pyrostatin A	Pyrostatin A methyl ester	Pyrostatin B
3	3.31(1H, br d, 15.0)	3.39(1H, br d, 14.9)	3.30(1H, ddd, 14.0, 8.6, 5.0)
	3.45(1H, ddd, 15.0, 2.4, 2.4)	3.49(1H, ddd, 14.9, 2.6, 2.6)	3.46(1H, ddd, 14.0, 5.6, 5.6)
4	4.54(1H, ddd, 2.4, 2.4, 2.4)	4.63(1H, ddd, 2.6, 2.6, 2.6)	2.07~2.19(2H, m)
5	4.05(1H, dd, 2.4, 2.4)	4.43(1H, dd, 2.6, 2.6)	4.07(1H, dd, 5.6, 5.6)
6	2.30(3H, s)	2.33(3H, s)	2.24(3H, s)
7-OCH <sub>3</sub>		3.83(3H, s)	

TABLE 3  
<sup>13</sup>C NMR data of pyrostatins in D<sub>2</sub>O.

Carbon	$\delta_{\text{C}}$ ppm (125 MHz)		
	Pyrostatin A	Pyrostatin A methyl ester	Pyrostatin B
2	161.3(s)	161.4(s)	161.2(s)
3	43.4(t)	42.2(t)	38.0(t)
4	60.2(d)	58.2(d)	22.1(t)
5	60.6(d)	56.9(d)	53.9(d)
6	18.8(q)	17.8(q)	18.9(q)
7	175.1(s)	169.9(s)	177.4(s)
7-OCH <sub>3</sub>		53.6(q)	

(C-2), 43.4 (C-3), 60.2 (C-4) and 175.1 (C-7) ppm. Since the NOE was observed between the methyl protons at  $\delta_{\text{H}}$  2.30 (6-H<sub>3</sub>) ppm and the methine proton at  $\delta_{\text{H}}$  4.05 (5-H) ppm, it was clear that they were adjacent to each other in the pyrrolidine ring. The presence of a carboxyl group was confirmed by the preparation of pyrostatin A methyl ester. From the above results, the structure of pyrostatin A was determined to be 4-hydroxy-2-imino-1-methylpyrrolidine-5-carboxylic acid (Figure 1). The absolute configuration remains to be determined.

The molecular weight and formula of pyrostatin B were elucidated as C<sub>6</sub>H<sub>10</sub>N<sub>2</sub>O<sub>2</sub> (MW 142) from the FAB-MS peak at  $m/z$  143 (M+H)<sup>+</sup>, HRFAB-MS [found:  $m/z$  143.0821 (M+H)<sup>+</sup>, calcd:  $m/z$  143.0819 for C<sub>6</sub>H<sub>11</sub>N<sub>2</sub>O<sub>2</sub>] and <sup>1</sup>H and <sup>13</sup>C NMR spectra of pyrostatin B (Tables 2 and 3). The UV and IR spectra, and the <sup>1</sup>H and <sup>13</sup>C NMR

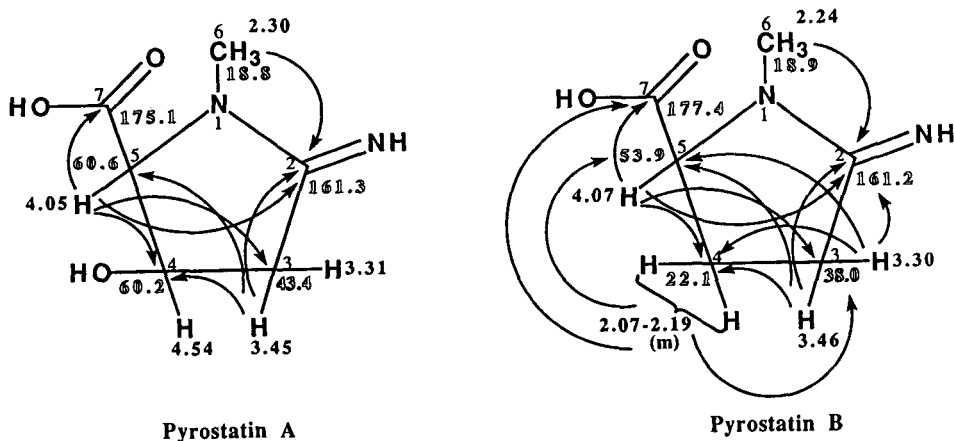


FIGURE 4  $^1\text{H}$ - $^{13}\text{C}$  correlations for pyrostatins A and B by HMBC experiments.

spectra of pyrostatin B were similar to those of pyrostatin A. Pyrostatin A showed a methine signal having a hydroxyl group at  $\delta_{\text{H}}$  4.54 (4-H),  $\delta_{\text{C}}$  60.2 (C-4) ppm, but this corresponding signal was not observed in the  $^1\text{H}$  and  $^{13}\text{C}$  NMR spectra of pyrostatin B. Instead of this signal, an additional methylene signal appeared at  $\delta_{\text{H}}$  2.07–2.19 (4-H<sub>2</sub>),  $\delta_{\text{C}}$  22.1 (C-4) ppm. Consequently, it was determined that pyrostatin B was 4-deoxypyrostatin A or 2-imino-1-methylpyrrolidine-5-carboxylic acid (Figure 1).

2-Iminopyrrolidine-5-carboxylic acid moiety has been found in some antibiotics, kikumycin A,<sup>9</sup> LL-BM123 $\alpha$ <sup>10</sup> and TAN-868A,<sup>11</sup> however, its 1-methyl derivative is a novel structure.

TABLE 4  
Inhibitory activity of various inhibitors against glycosidases

Inhibitor	$\text{IC}_{50}$ ( $\mu\text{g}/\text{ml}$ )			
	Sialidase <sup>a</sup>	$\beta$ -D-Galactosidase <sup>b</sup>	$\alpha$ -D-Mannosidase <sup>c</sup>	<i>N</i> -acetyl- $\beta$ -D-Glucosaminidase <sup>d</sup>
Siastatin B	3.0	>100	>100	>100
Pyridindolol	>100	1.8	>100	>100
Mannostatin A	>100	>100	0.02	>100
Mannostatin B	>100	>100	0.02	>100
Nagstatin	>100	>100	>100	0.002
Pyrostatin A	>100	>100	>100	0.45
Pyrostatin B	>100	>100	>100	0.82

<sup>a</sup>*Clostridium perfringens*, <sup>b</sup>bovine liver, <sup>c</sup>rat epididymis, <sup>d</sup>hog kidney



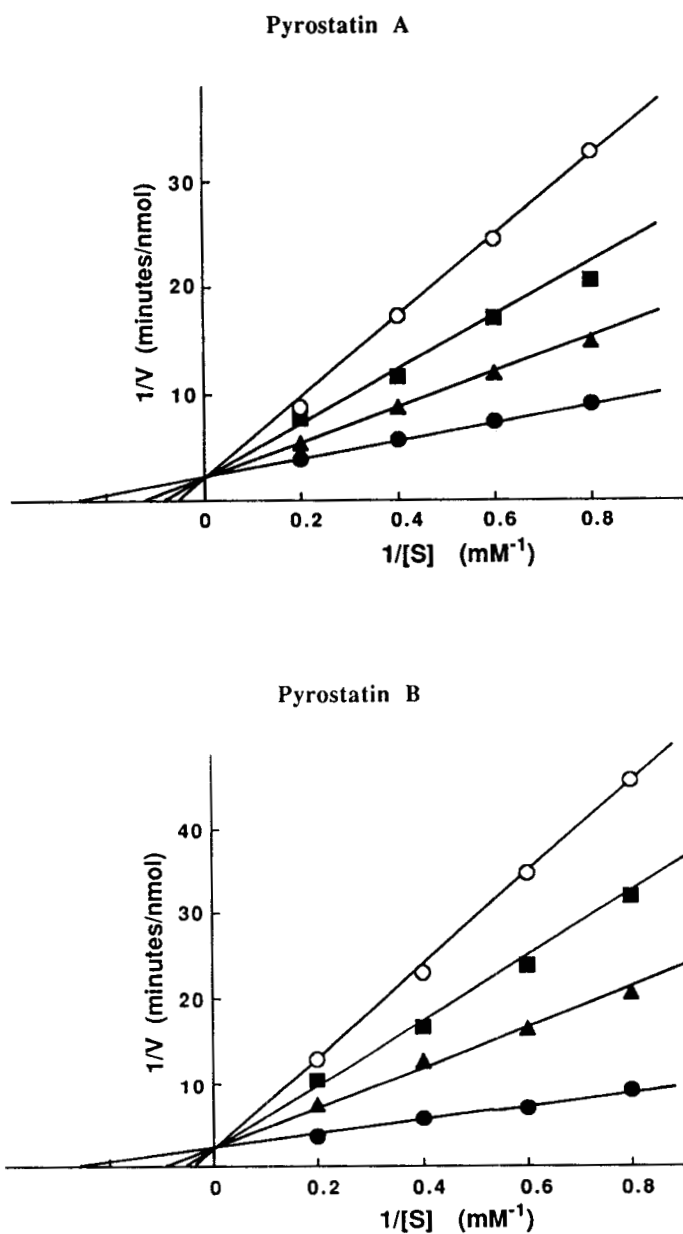


FIGURE 5 Lineweaver-Burk plots for inhibition of GlcNAc-ase by pyrostatins A and B. Pyrostatin A; ○ I=1.0  $\mu\text{g/ml}$ , ■ I=0.5  $\mu\text{g/ml}$ , ▲ I=0.25  $\mu\text{g/ml}$ , ● I=0  $\mu\text{g/ml}$ . Pyrostatin B; ○ I=1.6  $\mu\text{g/ml}$ , ■ I=0.8  $\mu\text{g/ml}$ , ▲ I=0.4  $\mu\text{g/ml}$ , ● I=0  $\mu\text{g/ml}$ .

### Biological Activities of Pyrostatins A and B

As shown in Figure 5, the inhibitions of pyrostatins A and B are competitive with substrate. The  $K_i$  values of pyrostatins A and B are  $1.7 \times 10^{-6}$  M and  $2.0 \times 10^{-6}$  M, respectively. The inhibitory spectrum against various glycosidases of the inhibitors which we have found in microbial culture fluids is shown in Table 4. Siastatin B<sup>12</sup> is a specific inhibitor against sialidase, pyridindolol<sup>13</sup> against  $\beta$ -D-galactosidase, manostatins A and B<sup>14</sup> against  $\alpha$ -D-mannosidase, nagstatin<sup>5,6</sup> and pyrostatins A and B against *N*-acetyl- $\beta$ -D-glucosaminidase, respectively. Pyrostatins A and B had no significant antimicrobial activity at 100  $\mu$ g/ml and showed no toxic indications after iv injection in mice at a dose of 100 mg/kg.

Among the most effective glycosidase inhibitors, are some polyhydroxylated piperidines and polyhydroxylated pyrrolidines.<sup>15</sup> Moreover, amidine derivatives of sugars whose structure, shape and charge closely resemble the transient glycosyl cation have been shown to be potent and broad spectrum inhibitors of glycosidases.<sup>16,17</sup>

### References

1. Alhadeff, J.A. and Holzinger, R.T. (1982) *Biochem. Med.*, **27**, 214.
2. Drexler, H.G., Gaedicke, G. and Minowada, J. (1983) *Leukemia Res.*, **7**, 611.
3. Pluncinsky, C., Propok, J.J., Alhadeff, M.D. and Alhadeff, J.A. (1986) *Cancer*, **58**, 1484.
4. Woynarowska, B., Wikiel, H., Sharma, M., Carpenter, N., Fleet, G.W.J. and Bernacki, R.J. (1992) *Anticancer Research*, **12**, 161.
5. Aoyagi, T., Suda, H., Uotani, K., Kojima, F., Aoyama, T., Horiguchi, K., Hamada, M. and Takeuchi, T. (1992) *J. Antibiotics*, **45**, 1404.
6. Aoyama, T., Naganawa, H., Suda, H., Uotani, K., Aoyagi, T. and Takeuchi, T. (1992) *J. Antibiotics*, **45**, 1557.
7. Tarentino, A.L. and Maley, F. (1972) *Meth. Enzymol.*, **28**, 772.
8. Shirling, E.B. and Gottlieb, D. (1966) *Int. J. Syst. Bacteriol.*, **16**, 313.
9. Takahashi, T., Sugawara, Y. and Suzuki, M. (1972) *Tetrahedron Lett.*, 1873.
10. Ellestad, G.A., Martin, J.H., Morton, G.O., Sassiver, M.L. and Lancaster, J.E. (1977) *J. Antibiotics*, **30**, 678.
11. Takizawa, M., Tsubotani, S., Tanida, S., Harada, S. and Hasegawa, T. (1987) *J. Antibiotics*, **40**, 1220.
12. Umezawa, H., Aoyagi, T., Komiya, T., Morishima, H., Hamada, M. and Takeuchi, T. (1974) *J. Antibiotics*, **27**, 963.
13. Aoyagi, T., Kumagai, M., Hazato, T., Hamada, M., Takeuchi, T. and Umezawa, H. (1975) *J. Antibiotics*, **28**, 555.
14. Aoyagi, T., Yamamoto, T., Kojiri, K., Morishima, H., Nagi, M., Hamada, M., Takeuchi, T. and Umezawa, H. (1989) *J. Antibiotics*, **42**, 883.
15. Eis, M.J., Rule, C.J., Wurzburg, B.A. and Ganem, B. (1985) *Tetrahedron Lett.*, **26**, 5397.
16. Pan, Y.T., Kaushal, G.P., Papandreou, G., Ganem, B. and Elbein, A.D. (1992) *J. Biol. Chem.*, **267**, 8313.
17. Tong, M.K., Papandreou G. and Ganem, B. (1990) *J. Am. Chem. Soc.*, **112**, 6137.